Journal of Non-Crystalline Solids 377 (2013) 34–38

Contents lists available at ScienceDirect

Journal of Non-Crystalline Solids

journal homepage: www.elsevier.com/locate/jnoncrysol

Structure of As_2Se_3 and As – Se network glasses: Evidence for coordination defects and homopolar bonding

M. Bauchy, M. Micoulaut *

Laboratoire de Physique Théorique de la Matière Condensée, Université Pierre et Marie Curie, Boite 121, 4, Place Jussieu, 75252 Paris Cedex 05, France

ARTICLE INFO

Article history:
Received 5 October 2012
Received in revised form 10 December 2012
Available online 4 February 2013

Keywords:
As_2Se_3;
As – Se;
Ab initio simulations;
Rigidity theory

ABSTRACT

The structural properties of As_2Se_3 and $AsSe_4$ glasses are investigated using the First Principles Molecular Dynamics. The results show an excellent agreement with measured structural properties in real and reciprocal space (total structure factors and total pair distribution functions, differential pair correlation functions). The analysis of the detail of the structure shows that homopolar As – As not only exist in the stochiometric compound but also for chalcogen rich compositions. Furthermore, coordination defects consisting of four-fold As and 1-fold Se are found to be of about 5–9%. Their topological nature, their evolution with temperature, as well as their contribution to the understanding of floppy to rigid transitions are discussed.

1. Introduction

The molecular structure of As_xSe_{1-x} glasses at $x<0.4$ has been widely described as a random network where Se chain fragments are crosslinked by pyramidal $AsSe_{3/2}$ units [1–3]. The resulting global topology and connectivity of the network appear to be substantially changed with As composition x, resulting in an important increase of the network mean coordination number $\bar{r}$ which manifests in the important variation of the glass transition temperature [4]. Anomalies have been reported as a function of As concentration, and these have been interpreted as the manifestation of a floppy to rigid transition [5] so that the As_xSe_{1-x} glasses have become an interesting benchmark system for approaches using rigidity theory. Indeed, based on topological constraint counting [6,7] where nearest-neighbor forces (stretching and bending) are considered, a network becomes isostatically rigid when the number of constraints n_c associated with these forces exactly balance the number of degrees of freedom, this condition being fulfilled at the network mean coordination number $\bar{r}=2.4$ which also corresponds to the well-known Maxwell stability criterion. With the assumption that 3-fold As crosslink the Se chains (in this case $\bar{r}=2+x$), the latter condition is supposed to be fulfilled for 40% As.

However, this simple picture has been challenged recently. First, calorimetric and optical probes have shown that onset of rigidity was taking place at lower As composition [8–10], suggesting the possibility of other local structures besides the pyramidal unit. More interestingly, an intermediate phase (IP) was identified [8] between 29% and 37% As, similarly to many other chalcogenide or oxide glasses [11–13]. This indicates that stressed rigidity percolates over a finite compositional interval and not at the single threshold value $\bar{r}=2.4$ [5]. According to recent theories, the IP seem to result from the self-organization of the network [14,15] which adapts under increasing cross-link concentration in order to reduce stressed rigidity. Secondly, several authors have reported [16–18] on viscosity or specific heat spectroscopy measurements showing that in the chalcogen rich domain a minimum in activation energies and fragility was obtained at $\bar{r}=2.3$ (30% As). The latter findings are in line with a Kirkwood–Keating model [19] showing that stress-free glasses in the IP have a minimum in activation energy for viscous flow. Last but not least, the maximum in glass transition temperature observed at 40% As which had been interpreted for many years as the manifestation of a rigidity transition [5] or a dimensional transition [20] seems to be the only signature of a nanoscale phase separation as extensively discussed in [21]. The occurrence of this stress-driven phase is due to the growing presence of As – As bonds which segregate from the network backbone by forming either isolated As_4Se_4 or ethylene-like units [22], resulting in a decrease of the network connectivity after the steady growth for $x<0.4$, thus maximizing some physical and chemical properties.

Taken together, these results reveal that the understanding of the structural and dynamic properties of As_xSe_{1-x} is certainly more complicated than in other chalcogenides [14]. The detection of the IP from calorimetric probes appears furthermore to be extremely sensitive to impurities and inhomogeneities [23]. Moreover, As – Se glasses being optically sensitive, non-reasoned sample handling can lead to misleading or wrong conclusions. Effects of uncontrolled aging on rigidity and calorimetric properties have been recently carefully reviewed [24].

Given these new results on a system of technological importance, there is space for additional studies, and especially for investigations using molecular simulations. These allow to propose accurate models that can serve for a reinterpretation of the accumulated experimental data. On the molecular structure in the short and intermediate range,

---

* Corresponding author.
E-mail address: mmi@lptl.jussieu.fr (M. Micoulaut).

0022-3093/$ – see front matter © 2013 Elsevier B.V. All rights reserved.
http://dx.doi.org/10.1016/j.jnoncrysol.2013.01.019

little is known although it is to be expected that structural defects occur as in other chalcogenides [25]. This is the purpose of the present contribution. We investigate by the First Principles Molecular Dynamics (FPMD) two compositions in the amorphous As – Se system: the stoichiometric As_2Se_3 and the chalcogen rich $AsSe_4$. The former will be extensively discussed while the latter will serve only at some specific points for comparison. Details on the structural properties of amorphous $AsSe_4$ will be presented elsewhere [26]. Results show that the network is made indeed of a majority of 3-fold coordinated As and 2-fold coordinated Se. However, an important fraction of homopolar As – As bonds are found, and this even for the selenide rich composition, together with 4-fold coordinated As in a tetrahedral geometry. No dimensional changes are obtained, the network of both compositions being fully 3D, as detected from the FPMD snapshots (Fig. 1). It should be noted that previous simulations have been reported on the stoichiometric amorphous system using either approximate ab initio schemes [27] or classical Molecular Dynamics [28]. Here we report on the first full density functional theory based simulation of amorphous As_2Se_3 using plane wave basis sets. Studies using this scheme have been performed only in the liquid state on very small system sizes [29].

2. Computational details

First principles simulations [30] were performed on As_2Se_3 and $AsSe_4$ systems consisting of 200 atoms. A periodically repeated cubic cell was used, corresponding to the number density of the glasses [8]. The electronic structure was described within density functional theory and evolved self-consistently during the motion. Valence electrons were treated explicitly, in conjunction with norm conserving pseudopotentials to account for core–valence interactions [31]. The wave functions were expanded at the Γ point of the supercell and the energy cutoff was set at 20 Ry. Most of the features of the simulation (fictitious mass, time step, exchange–correlation scheme, generalized gradient approximation) are identical to the one used in previous simulations on Ge – Se liquids and glasses [32]. All trajectories were accumulated over 25 ps. At 1200 K, four uncorrelated configurations separated by 5 ps have been selected to provide starting sets of coordinates. These have been quenched individually by steps (800 K, 600 K) to the glass. Data have been collected over these four independent quenches.

3. Results

In Fig. 2 the total structure factor $S_T(k)$ for amorphous As_2Se_3 is represented, and compared. It appears that our obtained $S_T(k)$ is improved for all wavevectors for the stoichiometric compound when compared to experimental data [33] and to the previous simulations [27,28]. The two principal peaks at 2.2 $Å^{-1}$ and 3.7 $Å^{-1}$ are very well reproduced, and also the peaks at higher k ($k > 6$ Å), in contrast with [27]. Note that the first sharp diffraction peak, while rather small in experiments [35], reduces in the simulations to a simple shoulder on the low wavevector side of the main peak. On the other hand, one notices that the force field used in classical Molecular Dynamics [28] fails to reproduce the main features of the measured structure factor.

Fig. 3 displays structural correlations in real space for As_2Se_3, and the positive conclusions holding for $S_T(k)$ are still valid. While panel a shows indeed that the present simulation agrees, again, very well with respect to experiments, similar to [27] and in contrast with [28], differential pair distribution functions obtained from anomalous X-ray scattering can be also very well reproduced [35]. The decomposition into pairs (panel b) displays some interesting features. As one can see, amorphous As_2Se_3 shows a prepeak at 2.35 Å and 2.59 Å in the Se – Se and As – As partials, respectively. These can be unambiguously attributed to homopolar bonds, whereas the main peak at 3.75 Å is related to the Se – Se distance being part the pyramidal $AsSe_{3/2}$ unit (experimentally, one has 3.64 Å [35]). In $g_{AsAs}(r)$, the main peak at 3.70 Å is associated with As – As correlations between two pyramids as also proposed by Hosokawa and co-workers [35,36]. Finally, the As – Se pair distribution function shows a sharp peak at 2.46 Å corresponding to the As – Se bond distance. These obtained bond distances are found to be in excellent agreement with those determined experimentally: 2.42 Å for As – Se, and 3.7 Å for the secondary peak from neutron [34], and 2.42 Å for As – Se from X-ray diffraction [35,36] It should be noted that because the homopolar bond distances are very close to the latter As – Se distance, they are not visible in the total pair distribution function (Fig. 3a), as they are overwhelmed by the high intensity of the first peak of $g_{AsSe}(r)$, as shown in Fig. 3b. From this figure, it appears furthermore that, surprisingly, homopolar As – As are already present in the 20% As glass $AsSe_4$ (broken red line).

From the partials displayed in Fig. 3, the corresponding coordination numbers can be computed by integrating the pdfs up to their first minimum r_m. These are equal to n_{AsAs} ($r_m = 2.93$ Å) = 0.64, n_{SeAs}

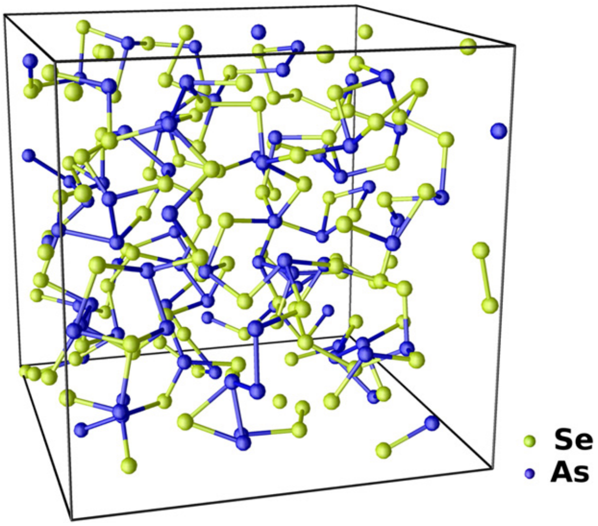

Fig. 1. A snapshot of a simulated amorphous As_2Se_3. Note the presence of homopolar As – As bonds, Se – Se chains and coordination defects.

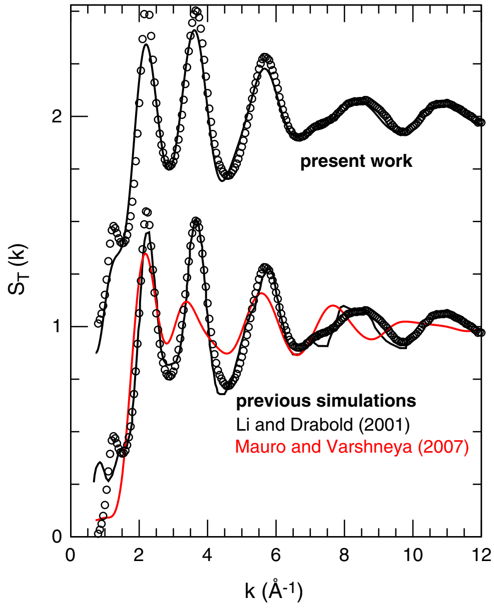

Fig. 2. Total simulated structure factor $S_T(k)$ of amorphous As_2Se_3 (black solid line, top) compared to previous simulations (bottom) from Li and Drabold (black, [27]) and Mauro and Varshneya (red, Fourier transform of the pair distribution function reported in [28]). All simulated functions are compared to experimental data (circles, [33]).

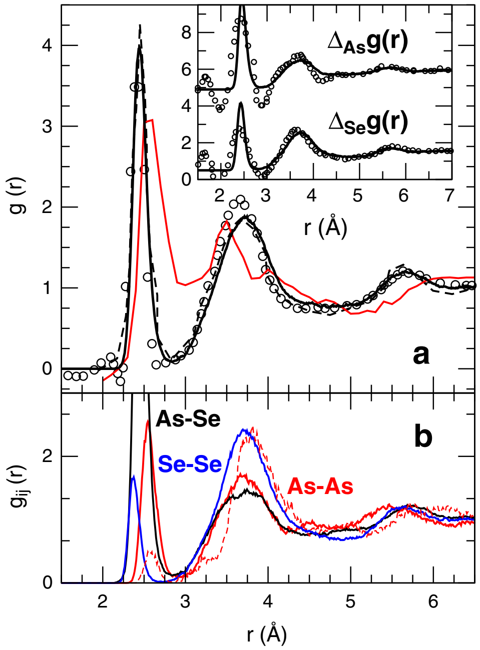

Fig. 3. a) Total simulated distribution function $g(r)$ of amorphous As_2Se_3 (solid line) compared to previous simulations from Li and Drabold (broken curve, [27]) and Mauro and Varshneya (red curve, [28]). All simulated functions are compared to experimental data (circles, [34]). The inset shows computed partial differential pair distribution functions $\Delta_{As}g(r)$ and $\Delta_{Se}g(r)$ (solid lines), compared to experimental data (circles) obtained from anomalous X-ray scattering [35]. b) Computed pair distribution $g_{ij}(r)$ of amorphous As_2Se_3: As – As (red), As – Se (black) and Se – Se (blue), and amorphous $AsSe_4$: As – As (thin broken red curve).

($r_m = 2.87$ Å) = 1.59 and finally n_{SeSe} ($r_m = 2.71$ Å) = 0.42. One has furthermore $n_{AsSe} = \frac{3}{2} n_{SeAs} = 2.38$. This leads to coordination numbers equal to $n_{As} = 3.02$, $n_{Se} = 2.01$ and $\bar{r} = 2.41$ on average, a result which clearly matches to what is expected from $AsSe_{3/2}$ pyramids cross-linking Se chains. However, inspection of the local topology through the calculation of the statistics of coordination numbers computed at each relevant r_m modifies this simple picture as a distribution of species with coordination number r_i is found (Table 1). While As has indeed on average 3 neighbors from the integration of g_{AsAs} and g_{AsSe} (see above), it appears that defect coordinated species exist with 4-folded As^{IV}. Similarly, terminal (one-fold) selenium Se^{I} is found. The concentration x_i of these species changes slightly as the As composition is changed, e.g. As^{IV} increases from 5.4% to 9.2% as one moves from $AsSe_4$ to As_2Se_3. From the concentration x_i of the r_i-coordinated species, we determine the same network mean coordination number ≡ 2.41 as above, and a number of constraints per atom of $n_c = 3.05$.

4. Discussion

The present results alters the traditional view of a chalcogen rich As – Se glassy structures consisting of randomly cross-linked pyramids undergoing dimensional changes. We do find indeed that homopolar As – As bonds not only do exist in the stoichiometric compound (As_2Se_3) but also at low As composition (20%). In this respect, the simulated structures from FPMD disagree with those obtained from Reverse Monte Carlo (RMC) [34] but also with those generated from Classical Molecular Dynamics [28]. For both, no evidence for homopolar bonds was found in As_2Se_3 although As – As bonds have an explicit Raman signature [22]. Experimentally, it has been stated that such homopolar bonds can be either part of ethylene-like $As_2Se_{4/2}$ polymeric chains as for example found in bulk AsSe glasses [37], or they can form part of an isolated cage-like molecular unit such as As_4Se_4 [24]. These signatures parallel those found in the isochemical P_xSe_{1-x} glasses where ethylene-like $P_2Se_{4/2}$ polymeric chains are observed once $x > 0.25$ [38]. Isolated As_4Se_4 units are not obtained in our simulated system (Fig. 1) although one must stress that the small system size probably does not warrant that there are none of them. It should finally be noted that, in contrast with $GeSe_2$ [32], the fraction of homopolar bondings (here As – As as compared to Ge – Ge) increases in the liquid (Fig. 4), as independently indicated by the broadening of the differential pair correlation function $\Delta_{As}g(r)$ with temperature [35].

Table 1
Coordination numbers statistics, mean coordination number $\bar{r}$, and number of constraint n_c in amorphous $AsSe_4$ and As_2Se_3. A cut-off distance of 2.82 Å has been used.

	r_i	1	2	3	4	5	$\bar{r}$	n_c
As_2Se_3	As		0.7	89.6	9.2	0.5	2.41	3.05
	Se	5.0	93.9	1.1				
$AsSe_4$	As		0.2	94.3	5.4	0.6	2.17	2.47
	Se	5.9	93.5	0.6				

Fig. 4 provides some additional insight into the network topology. It is found that the liquid can contain a large fraction of As^{IV} and this even down to the supercooled liquid state (600 K, i.e. $T/T_g = 1.28$ [8]).

We then ask the question whether there is a link between mis-coordination and homopolar bonding in As_2Se_3. For terminal Se^{I}, we find a ratio of 1:1 for Se – Se^{I} and As – Se^{I} bonds respectively. For As^{IV}, the ratio is of 2:1 for As^{IV} – As and As^{IV} – Se, whereas it is of about 1:1 for As^{III}, underscoring an increased tendency for mis-coordinated As to form homopolar bonds.

Finally, in order to characterize in a more deeper fashion the nature of the mis-coordinated As and its contribution in terms of rigidity, we use recently developed algorithms which enumerate e.g. angular (bending) constraints by computing the number of low angular standard deviations around a given atom. For details, the reader is referred to [39,40]. Let us only sketch the main ideas. In order to determine the local geometry and the number of constraints, we focus on the angular motion around a central atom 0 by following individually over the time trajectory angles defined by a set of N = 5 first neighbors: 102 (angle number 1, see Fig. 5), 103 (angle number 2), 203, etc. leading to N(N − 1)/2 = 10 possible angles. These serve as x-axis in Fig. 5. The angular motion over the trajectory leads to a bond angle distribution out of which a mean $<\theta>$ and a standard deviation σ_θ can be computed for each atom. The average over the whole system leads to a distribution of standard deviations [39] which have either low values (typically $\sigma_\theta \simeq 10°$) or high values ($\sigma_\theta > 20°$). These define intact or broken angular constraints, respectively. We find (Fig. 5b) that the As^{IV} has 6 low standard deviations (i.e. five independent constraints as also obtained directly from Maxwell constraint counting [7]) associated with a mean angle $<\theta> = 109°$ (Fig. 5a),

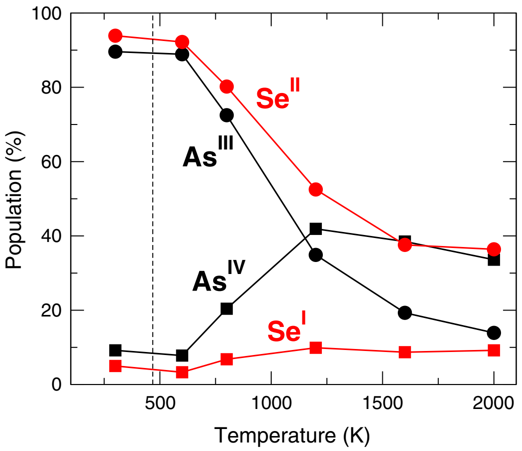

Fig. 4. Fraction of As and Se species in amorphous and liquid As_2Se_3 as a function of temperature. The broken vertical line is the experimental glass transition temperature [8].

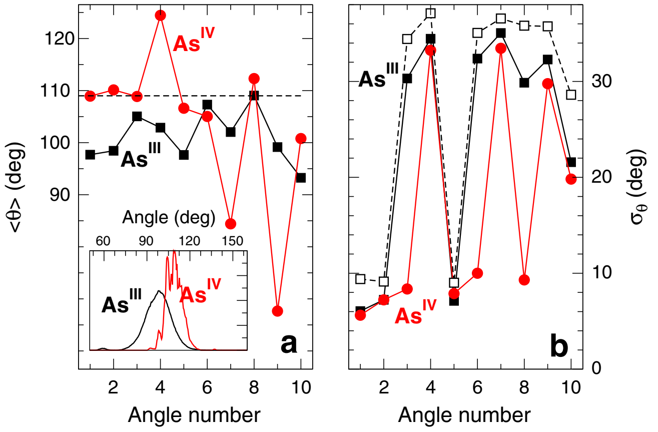

Fig. 5. Mean angle <θ> (a) and standard deviation σ_θ (filled symbols) of partial bond angle distributions (b) as a function of an arbitrary angle number for detected As^{III} (black) and As^{IV} species (red) in As_2Se_3. The σ_θ of As^{III} in $AsSe_4$ (open box, broken line) is also represented. The insert shows the bond angle distribution of such species.

indicative of a tetrahedral environment. On the other hand, the As^{III} atoms have only three intact constraints and a mean angle of 98°, exactly equal to the experimental estimate by Hosokawa et al. [35].

We now arrive to the question of the mechanical nature of As_2Se_3. Inspection of Fig. 5b indicates that not all the standard deviations are equal, i.e. the angular motion inside both the $AsSe_{3/2}$ pyramid and the tetrahedral $AsSe_{4/2}$ is non-symmetric, the angles involving the farthest atom (3rd neighbor in $AsSe_{3/2}$ and 4th one in $AsSe_{4/2}$) having an increased angular motion which give rise to an increased σ_θ. The spread over σ_θ for the relevant angles is found to be reduced when moving from As_2Se_3 to $AsSe_4$. Recently, it has been shown [40] that the same angular distorted motion was taking place for stressed rigid compositions of Ge–Se glasses, whereas all relevant σ_θ's were found to be nearly constant for floppy and IP compositions, similar to $AsSe_4$ (Fig. 5b). The presence of stress leads, in fact, to asymmetric bending motions inside $GeSe_{4/2}$ tetrahedra as additional cross-links imposes softer (angular) interactions to adapt which leads to increased angular excursions around the mean value. The present argument is in line with the well-known relationship between stressed rigidity and bond mismatch in simple bond networks [41]: atoms with a given coordination number cannot fulfill all their bonds at the same length because of a too high bond density or network connectivity. Given these facts and general comments, one arrives to the conclusion that some stress must be present in As_2Se_3 as it displays the same angular asymmetric motion as the stressed rigid $GeSe_2$. But at the same time, one obtains a structure which leads to a number of constraints corresponding to a nearly isostatic (optimally constrained) composition. Further developments and analyses are needed and being considered.

5. Summary and conclusion

In this contribution, we have computed and analyzed the structural properties of amorphous As_2Se_3. Effects of composition have been discussed by comparing with the chalcogenide rich $AsSe_4$ system. While the overall structural description is clearly improved with respect to previous modeling [27,28], we find that the glass network is made of a majority of pyramidal $AsSe_{3/2}$ units with features at the short range level (bond distances, bond angles) and intermediate range level ($S_T(k)$) in excellent agreement with experimental measurements. A large fraction of As–As homopolar bonds is found, even at low As composition, indicative of a possible reported nanoscale phase separation [22] once the As composition becomes close to 40%. Given the stoichiometry of As_2Se_3, the presence of such connections imposes that Se–Se homopolar bonds still exist, and these manifest by a prepeak in the Se–Se partial pair distribution function. In this respect, we stress that the present system bears similarities with another stochiometric chalcogenide, $GeSe_2$, for which such homopolar defects have been found both from theory [32] and experiment [25]. However, in contrast with the latter system, a detailed experimental analysis of amorphous As_2Se_3 from partial pair distribution functions or structure factors using e.g. isotopic substituted neutron diffraction (see however [35]) is lacking. Such needed measurements are welcome.

While As has a coordination number which is three on average, we also find that As_2Se_3 has coordination defects consisting of four-fold tetrahedral As^{IV} and terminal (1-fold) Se^{I}, their fraction being of about 5–9%. The fraction of As^{IV} is found to be highly temperature dependent as their fraction increases rapidly between 300 K and the melt at 800 K. Furthermore, the tendency to form homopolar bonds is increased in the presence of four-fold arsenic.

In conclusion, our study also shows that additional studies are needed to fully understand the connection of the structural properties with the onset of rigidity in As–Se glasses. A rigid intermediate phase has been reported between 29% and 37% As, in connection with the existence of a quasi-tetrahedral As unit [8]. The present investigation leads only to a minority of such structural motifs (5–9%) with a strong variation in the deep supercooled liquid. One has therefore to be careful with the proposed statistics as the corresponding calculated As^{IV} fraction could be different and affected by the computer timescale. Dimensional changes have been invoked to understand rigidity effects [16]. Unfortunately, no dimensional phase separation is found, both systems, $AsSe_4$ and As_2Se_3 being fully 3D. A study on larger system sizes could clarify this issue although it has been shown recently that the induced structural changes are minuscule [42].

The underlying driving force for the onset of rigidity and the location of the IP in As–Se remains therefore to be discovered, and one may at this point highlight the fact that the unusual presence of homopolar As–As bonds, especially in $AsSe_4$, may well be one of the possibilities. In fact, in the corresponding Ge_xSe_{1-x} systems, homopolar Ge–Ge bonds appear only in the IP [40], their important increase at higher Ge compositions being the result of stressed rigidity [21]. Here, as both compositions contain such homopolar defects, one arrives to the conclusion that $AsSe_4$ and As_2Se_3 must be more rigid than believed (Table 1), at least from the simple global counting argument [7] which leads to a rigidity transition for 40% As but unfortunately disagrees with the most recent experimental findings [8,16]. Finally, the increased angular distorted motion inside the $AsSe_{3/2}$ pyramid in As_2Se_3 is also an indirect evidence for stress, similarly to previous findings in Ge–Se network glasses [40]. In any case, an exact constraint counting appears to be challenging while the global one will need to be revisited, perhaps based on our obtained new structural information.

Acknowledgments

It is a pleasure to acknowledge stimulating discussions with G. Ferlat, S. Le Roux, C. Massobrio, N. Mousseau, P. Boolchand. Support from Agence Nationale de la Recherche (ANR) (grant no. 09-BLAN-0109-01) is gratefully acknowledged. GENCI (Grand Equipement National de Calcul Intensif) is acknowledged for supercomputing access.

References

[1] M.B. Myers, E.J. Felty, MRS Bull. 2 (1967) 535.
[2] Y. Sagara, O. Uemura, S. Okuyama, T. Satow, Phys. Status Solidi A 31 (1975) K33.
[3] E.D. Crozier, F.W. Lytle, D.E. Sayers, Can. J. Chem. 55 (1977) 1968.
[4] A.L. Renninger, B.L. Averbach, Phys. Rev. B 8 (1973) 1507.
[5] J. Wells, P. Boolchand, J. Non-Cryst. Solids 89 (1987) 31.
[6] J.C. Phillips, J. Non-Cryst. Solids 34 (1979) 155.
[7] M.F. Thorpe, J. Non-Cryst. Solids 55 (1983).
[8] D.G. Georgiev, P. Boolchand, M. Micoulaut, Phys. Rev. B 62 (2000) R9228.
[9] D.G. Georgiev, P. Boolchand, M. Micoulaut, J. Optoelectron. Adv. Mater. 4 (2002) 823.
[10] P. Chen, C. Holbrook, P. Boolchand, D.G. Georgiev, M. Micoulaut, Phys. Rev. B78 (2008) 224208.
[11] M. Micoulaut, M. Malki, D.I. Novita, P. Boolchand, Phys. Rev. B 80 (2009) 184205.

[12] D. Selvanathan, W.J. Bresser, P. Boolchand, Phys. Rev B 61 (2000) 15061.
[13] P. Boolchand, D.G. Georgiev, B. Goodman, J. Optoelectron. Adv. Mater. 3 (2001) 703.
[14] M. Micoulaut, J.C. Phillips, Phys. Rev. B 67 (2003) 104204.
[15] M. Micoulaut, Phys. Rev. B 74 (2006) 184208.
[16] G. Yang, O. Gulbiten, Y. Gueguen, B. Bureau, J.-C. Sangleboeuf, C. Roiland, E.A. King, P. Lucas, Phys. Rev. B 85 (2012) 144107.
[17] G. Yang, B. Bureau, T. Rouxel, Y. Gueguen, O. Gulbiten, C. Roiland, E. Soignard, J.L. Yarger, J. Troles, J.-C. Sangleboeuf, P. Lucas, E.A. King, P. Lucas, Phys. Rev. B82 (2010) 195206.
[18] J.D. Musgraves, P. Wachtel, S. Novak, J. Wilkinson, K. Richardson, J. Appl. Phys. 110 (2011) 063503.
[19] M. Micoulaut, J. Phys. Condens. Matter 22 (2010) 285101.
[20] K. Tanaka, Phys. Rev. B 39 (1989) 1270.
[21] P. Boolchand, D.G. Georgiev, T. Qu, F. Wang, L. Cai, S. Chakravarty, Comptes Rendus Chimie 5 (2002) 713.
[22] S. Mamedov, D.G. Georgiev, T. Qu, P. Boolchand, J. Phys. Condens. Matter 15 (2003) S2397.
[23] S. Bhosle, P. Boolchand, M. Micoulaut, C. Massobrio, Solid State Commun. 151 (2011) 1851.
[24] P. Chen, P. Boolchand, D.G. Georgiev, J. Phys. Condens. Matter 22 (2010) 065104.
[25] P.S. Salmon, I. Petri, J. Phys. Condens. Matter 15 (2003) S1509.
[26] M. Bauchy, J. Non-Cryst. Solids. (in press).
[27] J. Li, D.A. Drabold, Phys. Rev. B 64 (2001) 104206.
[28] J.C. Mauro, A.K. Varshneya, J. Non-Cryst. Solids 353 (2007) 1226.
[29] F. Shimojo, S. Munejiri, K. Hoshino, Y. Zempo, J. Phys. Condens. Matter 12 (2000) 6161.
[30] R. Car, M. Parrinello, Phys. Rev. Lett. 55 (1985) 2471.
[31] N. Trouiller, J.L. Martins, Phys. Rev. B 43 (1991) 1993.
[32] M. Micoulaut, R. Vuilleumier, C. Massobrio, Phys. Rev. B 79 (2009) 214204;
C. Massobrio, M. Micoulaut, P.S. Salmon, Solid St. Sci. 12 (2010) 199;
M. Bauchy, M. Micoulaut, M. Celino, M. Boero, S. Le Roux, C. Massobrio, Phys. Rev. B 83 (2011) 054201.
[33] S. Xin, P.S. Salmon, Phys. Rev. B 78 (2008) 064207.
[34] M. Fabian, E. Sváb, V. Pamukchieva, A. Szekeres, S. Vogel, U. Ruett, J. Phys. Condens. Matter 253 (2010) 012053.
[35] S. Howokawa, Y. Wang, W.-C. Pilgrim, J.-F. Bérar, S. Mamedov, P. Boolchand, J. Non-Cryst. Solids 352 (2006) 1517;
S. Hosokawa, Y. Kawakita, W.-C. Pilgrim, F. Hensel, J. Non-Cryst. Solids 293–295 (2001) 153.
[36] S. Hosokawa, Y. Sakaguchi, K. Tamura, J. Non-Cryst. Solids 150 (1992) 35.
[37] A. Sklenar, M. Vleck, P. Bezdicka, in: A. Helebrant, M. Maryska, S. Kasa (Eds.), Proc. 5th ESG Conference Glass Science and Technology for the 21st Century, C1, 1999, p. 99, (Prague).
[38] D.G. Georgiev, M. Mitkova, P. Boolchand, G. Brunklaus, H. Eckert, M. Micoulaut, Phys. Rev. B 64 (2001) 134204.
[39] M. Bauchy, M. Micoulaut, J. Non-Cryst. Solids 357 (2011) 2530.
[40] M. Bauchy, M. Micoulaut, M. Celino, M. Boero, S. Le Roux, C. Massobrio, Phys. Rev. B 83 (2011) 054201.
[41] N. Mousseau, M.F. Thorpe, Phys. Rev. B 52 (1995) 2660.
[42] M. Micoulaut, S. Le Roux, C. Massobrio, J. Chem. Phys. 136 (2012) 224504.